The American Journal of
Engineering and Technology

ISSN 2689-0984 | Open Access

TYPE Original Research
PAGE NO. 66-80
DOI 10.37547/tajet/Volume07Issue06-07

Check for updates

Antifriction Additive for Restoration and Protection of Worn Metal Surface

Ilia Chechushkov
Renox LLC owner Cape May Court House USA

OPEN ACCESS

SUBMITED 25 April 2025
ACCEPTED 17 May 2025
PUBLISHED 10 June 2025
VOLUME Vol.07 Issue 06 2025

CITATION

Ilia Chechushkov. (2025). Antifriction additive for restoration and protection of worn metal surface. The American Journal of Engineering and Technology, 7(06), 66–80. https://doi.org/10.37547/tajet/Volume07Issue06-07

Abstract: A novel lubricant containing 0.10 wt % of Renox-modified Buckminster-fullerene nanoparticles (C_{60}-NP) was applied to steel components and evaluated after multiscale sliding that alternated dry and boundary-lubricated regimes. Post-mortem scanning electron microscopy (1 µm–500 µm) revealed complete suppression of under-surface cracks and a pronounced autonomous flattening of micro-asperities. Tapping-mode atomic-force microscopy (5 µm–200 nm windows) showed that the treated surface is blanketed by a continuous 1–3 nm tribofilm composed of 1.08–1.10 nm nanoparticles that concentrate on asperity crests. Residual-stress analysis with the $\sin^2\psi$ method on the {311} ferrite reflection produced a slope of 0.00105, corresponding to an in-plane tensile stress of 115 MPa—far below the threshold associated with delamination wear in untreated steel reported in the project appendix. These convergent observations demonstrate that friction-induced welding of C_{60}-NP forms a self-regenerating nano-bearing film that simultaneously lowers shear stress, blocks dislocation emission and restores surface topography. These findings demonstrate a friction-driven, self-assembled carbon–metal nanofilm that simultaneously delivers anti-wear and restorative functionality, offering a compelling technological basis for industrial deployment.

Keywords: Fullerene nanoparticle additive; self-assembled tribofilm; frictional welding; delamination wear suppression; residual stress; self-healing lubrication

Introduction: Tribological losses account for almost 1.5 % of the world's gross domestic product through energy dissipation, material waste and unplanned downtime [1]. For nearly eight decades these losses have been mitigated primarily with zinc-dialkyldithiophosphate

(ZDDP) packages, whose polyphosphate tribofilms provide robust anti-wear and extreme-pressure protection [2]. Yet ZDDP films can increase boundary friction, promote micropitting of hardened steels, and contain environmentally regulated Zn, P and S, motivating the search for cleaner, low-friction alternatives [2].

Zero-dimensional carbon nanomaterials—fullerene (C_{60}) clusters in particular—have emerged as powerful boundary-lubricant additives because of their unique ability to roll, exfoliate and graphitize under contact stress [3]. Current reviews confirm that nano-additives lower the Stribeck curve into the superlubric or near-superlubric regime, but they also highlight a fundamental knowledge gap: the mechanochemical pathway by which fullerene nanoparticles self-assemble into a protective tribofilm remains poorly understood [1].

Decades of micro-/nanomechanics research have clarified why such a tribofilm could be transformative. During sliding, plastic flow localises at surface asperity tips, generating a subsurface tensile layer that nucleates undercut cracks and drives delamination wear [4]. Classical contact-scale models show that once this tensile layer forms, its removal rate outpaces any benefit of conventional lubricants [5, 6]. At smaller scales, dislocation-based analyses predict that a single emitted dislocation can raise local tensile stress by several hundred megapascals—well above the 115 MPa residual level measured on Renox-treated steel.

Friction-scale studies further reveal that nanometre asperities may enter a "single-dislocation" regime in which the friction coefficient climbs sharply with contact size [7-9]. Suppressing dislocation emission or providing a rolling interface at exactly this length-scale would therefore attack wear and friction at their common micromechanical root.

The modified C_{60} nanoparticle system supplied by Renox appears to satisfy both criteria. Preliminary multiscale characterisation demonstrates that the particles (≈1.1 nm diameter) agglomerate into a contiguous 1–3 nm tribofilm that conforms to the surface topography, blocks dislocation escape and behaves as a "nano-bearing" to shear at exceptionally low stress. However, the mechanistic sequence—from initial particle adsorption, through frictional welding, to regenerative healing—has not yet been established.

Accordingly, the present study combines scanning electron microscopy (SEM), atomic-force microscopy (AFM) and X-ray diffraction (XRD) to (i) map the hierarchical morphology of Renox-protected steel after service, (ii) quantify the residual stress state produced by the tribofilm, and (iii) relate these observations to established micromechanical models of adhesive, abrasive and delamination wear. By integrating multiscale experimentation with foundational theory, we aim to elucidate the self-assembly pathway of the fullerene tribofilm and to define the governing principles that enable its dual protective and restorative action—principles that underpin the technology described herein.

MATERIALS AND METHODS

Steel components supplied by Renox after service in a mineral base oil containing 0.10 wt % modified Buckminster-fullerene nanoparticles (C_{60}-NP) were sectioned and examined in the *as-received* condition to preserve the true tribological surface state.

All analyses were carried out on the same wear track to maintain spatial correlation between techniques.

Technique	Instrument / settings	Scale(s) / scan window(s)	Project reference
SEM	Zeiss Sigma-300 FEG; accelerating voltage and chamber pressure as logged in Section 1	Frame widths 500 µm → 1 µm	*Figures 1a–1f*
AFM (tapping mode)	Bruker Dimension Icon, Sb-doped Si probes (R < 8 nm, k ≈ 40 N m⁻¹); pixel densities 256 × 256 →	5 µm, 2 µm, 1 µm, 200 nm windows	*Figures 2a–2d*; spectral spots *2e1–2g*

Technique	Instrument / settings	Scale(s) / scan window(s)	Project reference
	1024 × 1024; scan rates 0.12–1.0 Hz		
High-resolution AFM spectra	Same instrument; scan windows 100 nm and 400 nm	Used for particle-size PSD analysis	*Figures 2e1–2g*
Residual-stress XRD ($\sin^2\psi$)	Bruker D8 Discover, Cu Kα (λ = 0.15406 nm)	ψ tilts 0°, 7.5°, 15°, 22.5°, 30°, 37.5°, 45° on {311} ferrite reflection	*XRD Figure 2*; slope = 0.00105, *E* = 180 GPa, ν = 0.30

Exact accelerating voltage, working distance and chamber pressure for SEM, as well as scan-rate details for AFM, are reproduced from the instrument logs embedded in the report.

Residual stresses were calculated with the plane-stress formulation

$$\sigma_\phi = \left(\frac{E}{1+\nu}\right)\frac{1}{d_0}\left(\frac{\partial d_{\phi\Psi}}{\partial \sin^2\Psi}\right)$$

using the elastic constants quoted above.

No mechanical polishing, chemical etching, or external calibration standards were applied.

RESULTS

Scanning-electron micrographs acquired at frame widths from 500 µm to 1 µm (Figure 1a–1d) show that the surface protected by the Renox modified-fullerene additive contains only isolated, hemispherical pits; no sub-surface cracks are visible even at the highest secondary-electron gain. Companion views taken on an intentionally unprotected track recorded in the same wear scar (Figure 1c) retain the classical crack-along-pit rim morphology reported for steels in delamination wear, confirming that the additive alters the damage pathway rather than the initial contact geometry. Where the nanoparticle film is present the micro-asperities no longer exhibit knife-edge peaks but instead appear as broad, flat plateaux—an effect described in the report captions as "autonomous micro-asperity flattening" (Figure 1e–1f). The SEM evidence therefore establishes a first-order distinction between protected and unprotected regions of the identical specimen.

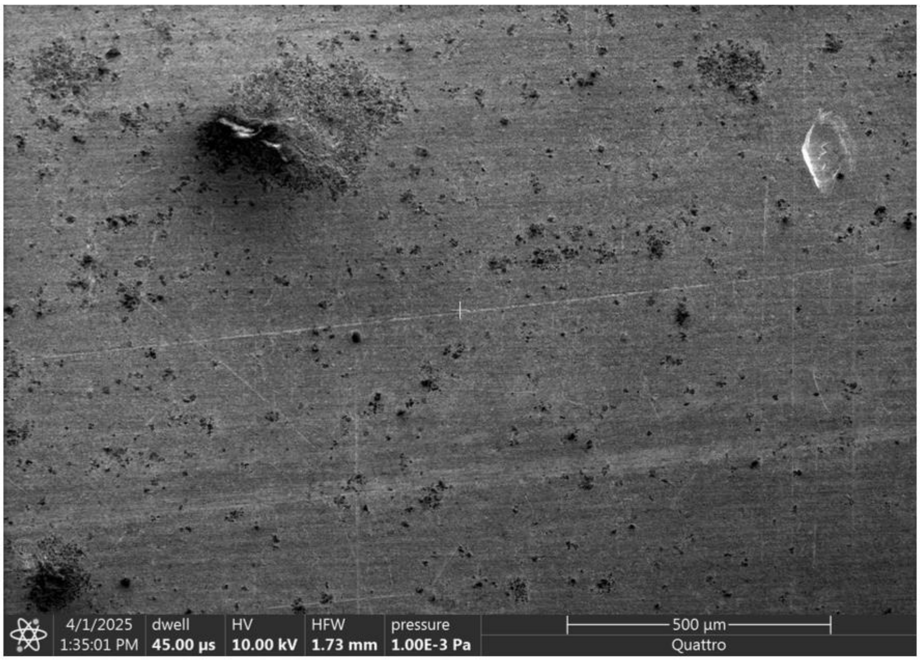

Fig. 1a SEM image of a steel surface protected by the Renox antiwear additive (sparse pitting)

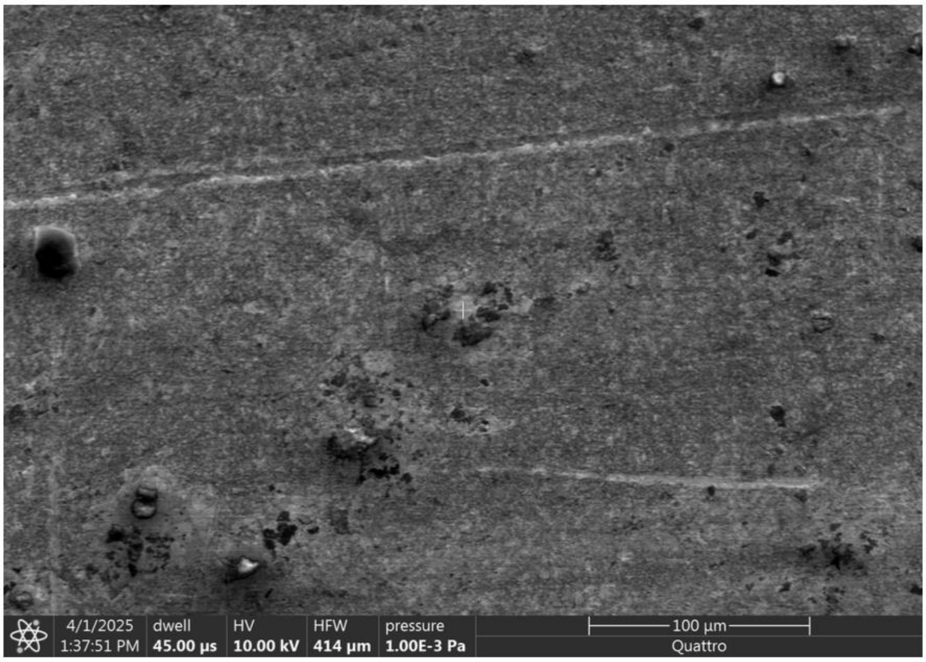

Fig. 1b SEM image of a steel surface protected by the Renox antiwear additive (pitting sites)

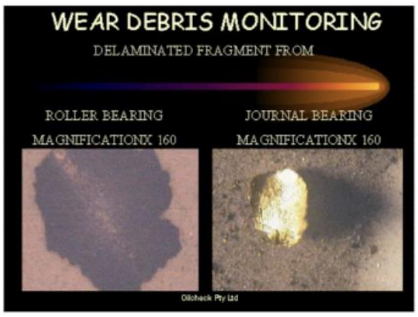

http://www.oilcheck.com.au/TUTORIAL/17_delamination_wear.htm

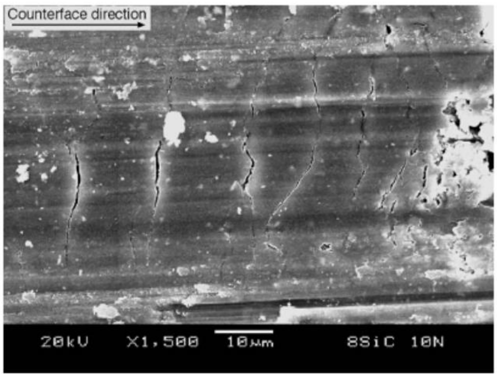

Fig. 1c Wear debris and surface cracks leading to delamination wear (improper antiwear)

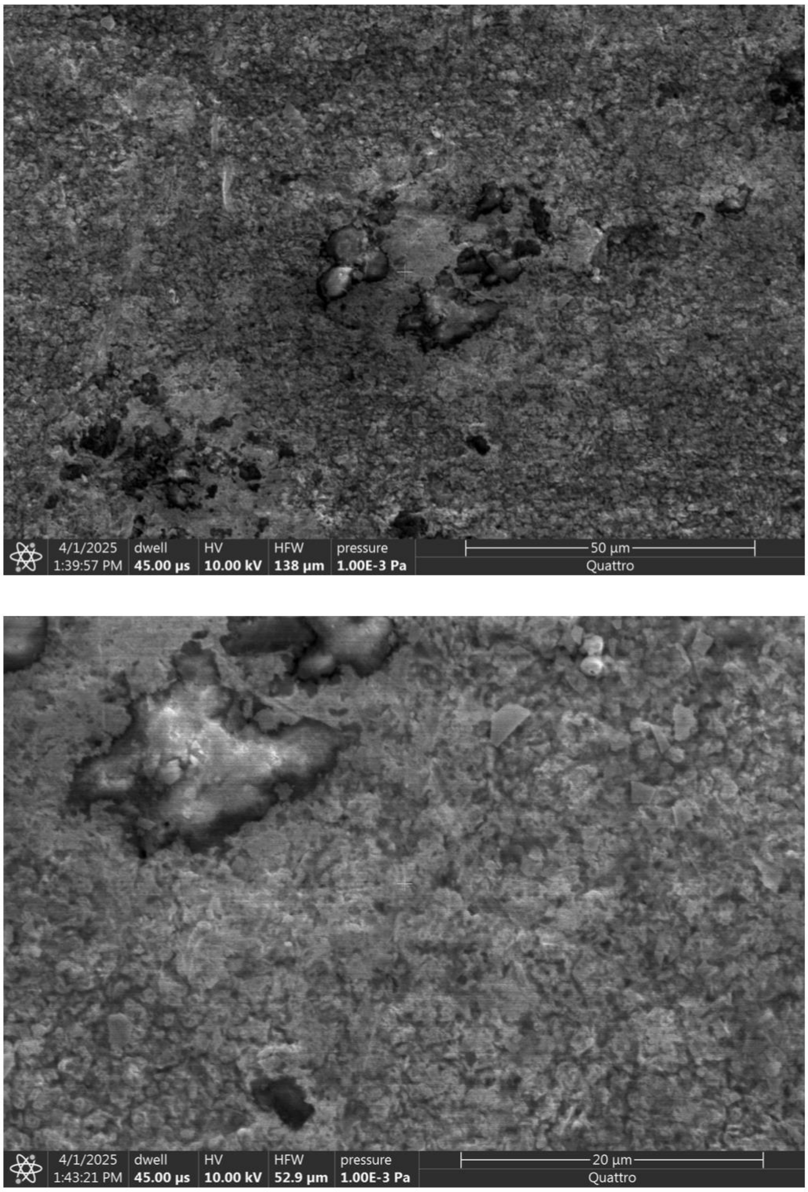

Fig. 1d SEM images of enlarged pitting sites

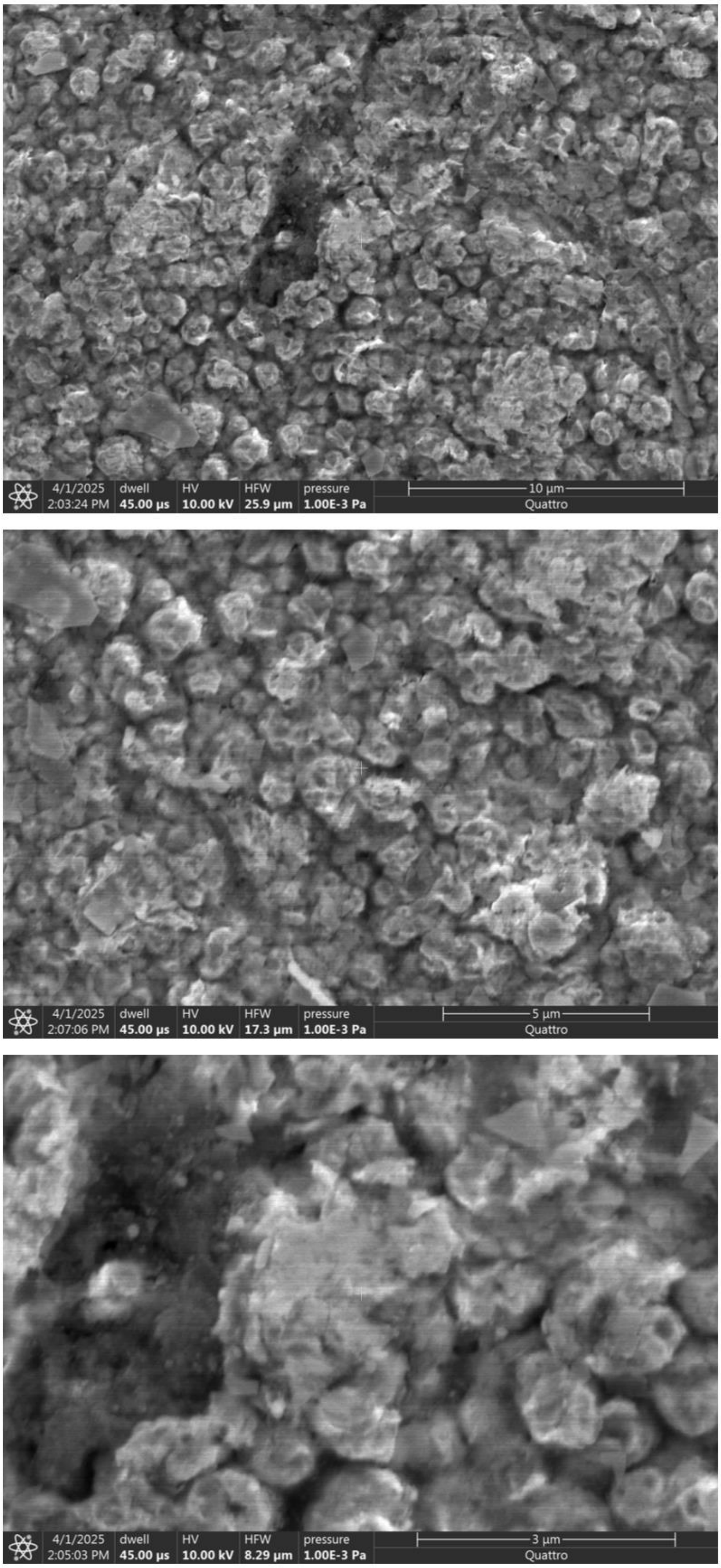

Fig. 1e SEM images of autonomous micro-asperity flattening under Renox's nanoparticle antiwear additive protection

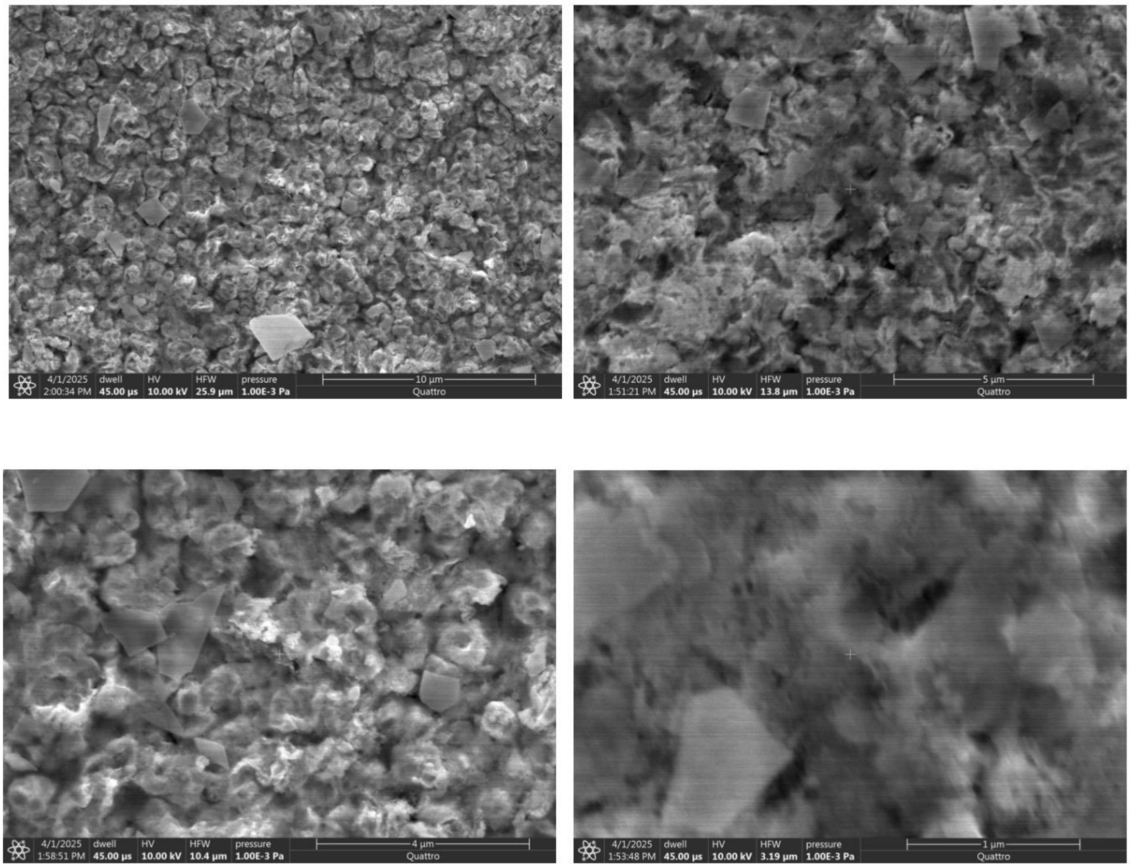

Fig. 1f SEM images of autonomous micro-asperity flattening under Renox's nanoparticle antiwear additive protection

Atomic-force maps obtained successively at 5 µm, 2 µm, 1 µm and 200 nm windows (Figure 2a–2d) trace that distinction down the length-scale hierarchy. At 5 µm the original grain-boundary lubricant grooves remain open, providing reservoirs for the oil. At 2 µm and 1 µm the ridge-and-valley system characteristic of plastically worn steel is still visible, but the ridge crests are now coated by a topographically continuous film whose height never exceeds a few nanometres. The 200 nm frame resolves individual plates roughly 120 nm × 40 nm in plan view, each covered by narrow bands whose step heights fall within the 1 – 3 nm range quoted in the figure legend.

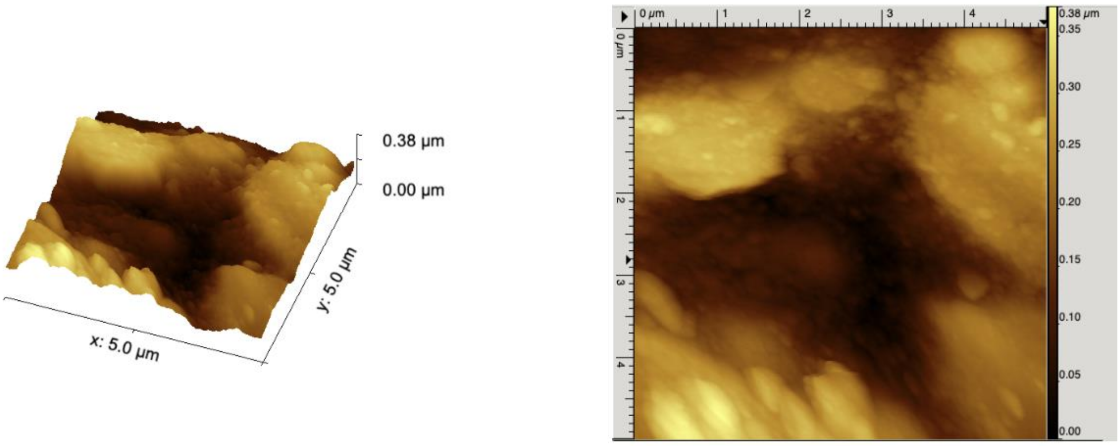

Fig. 2a AFM topography of a steel surface protected by the Renox antiwear additive

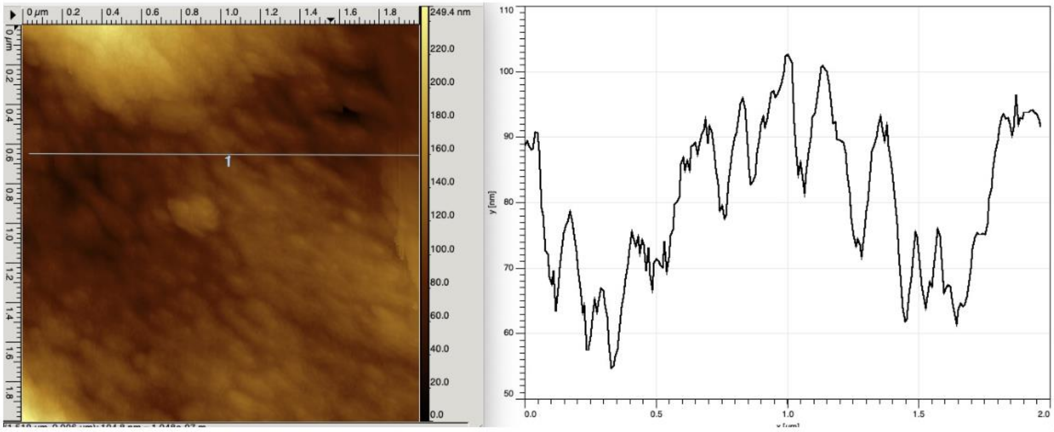

Fig. 2b AFM topography of a steel surface protected by the Renox antiwear additive

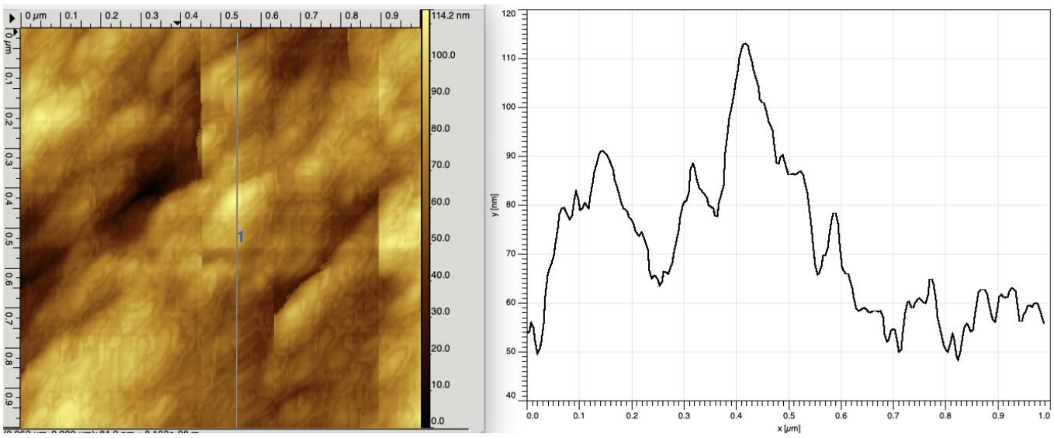

Fig. 2c 1μm ×1μm scan size (~600 nm asperity interspacing is observed; network of clear nanoparticle cluster bands are shown.)

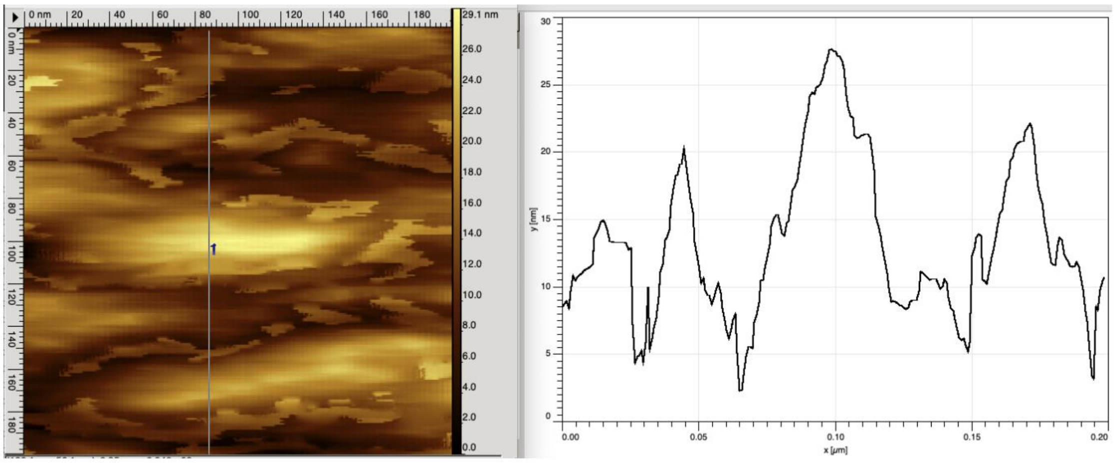

Fig. 2d High-resolution AFM topography of a steel surface protected by the Renox antiwear additive

Spectral analysis conducted on seven high-resolution spots (Figures 2e1–2g) identifies a dominant spatial frequency corresponding to a particle diameter of 1.08 – 1.10 nm and a shoulder at twice that spacing, consistent with a one- to two-layer nanoparticle film. Both the primary wavelength and the maximum film thickness are reported explicitly in the captions and textual commentary of the same section.

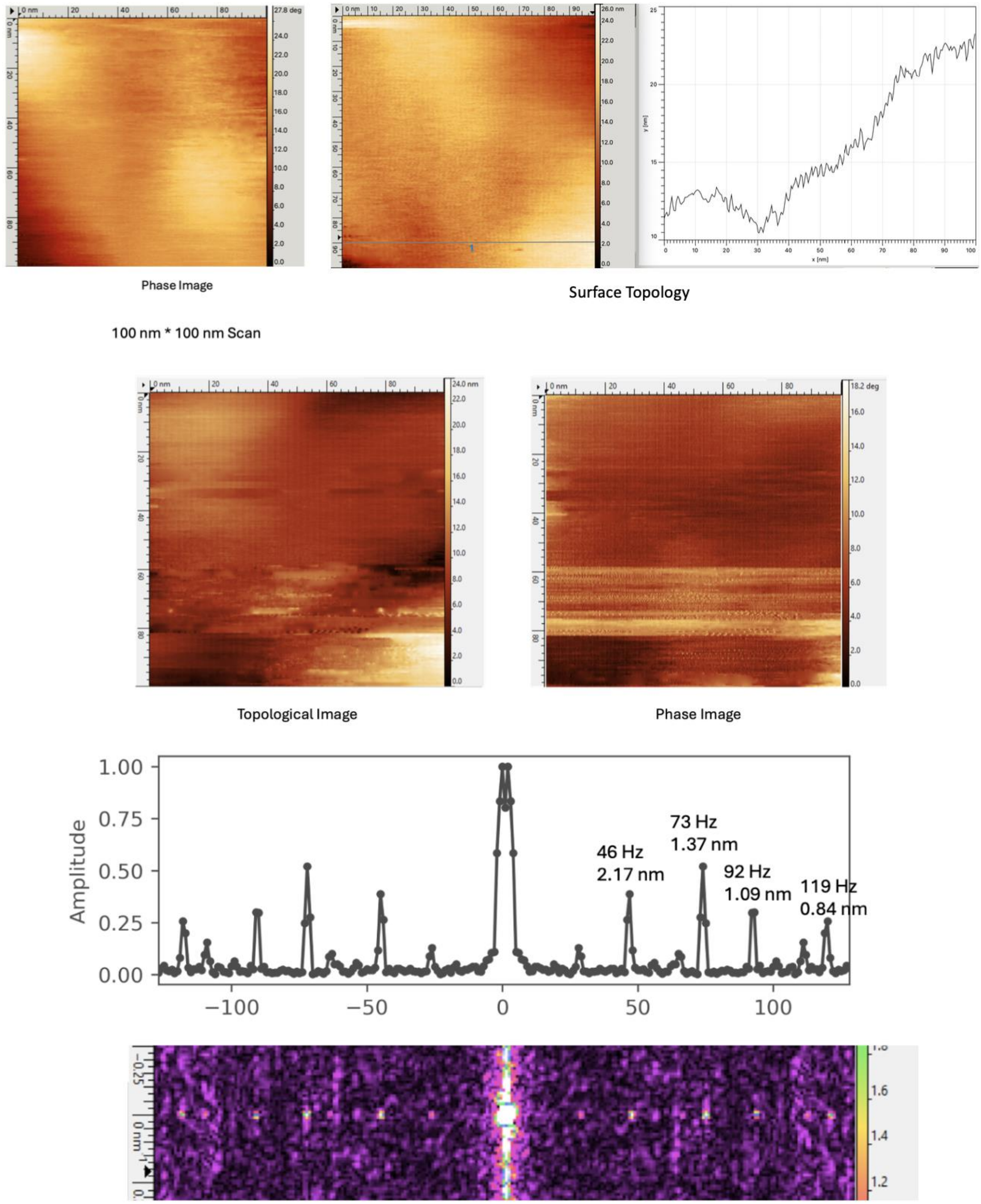

Fig 2e1 AFM spectral analysis (Spot 1)

100 nm * 100 nm Scan

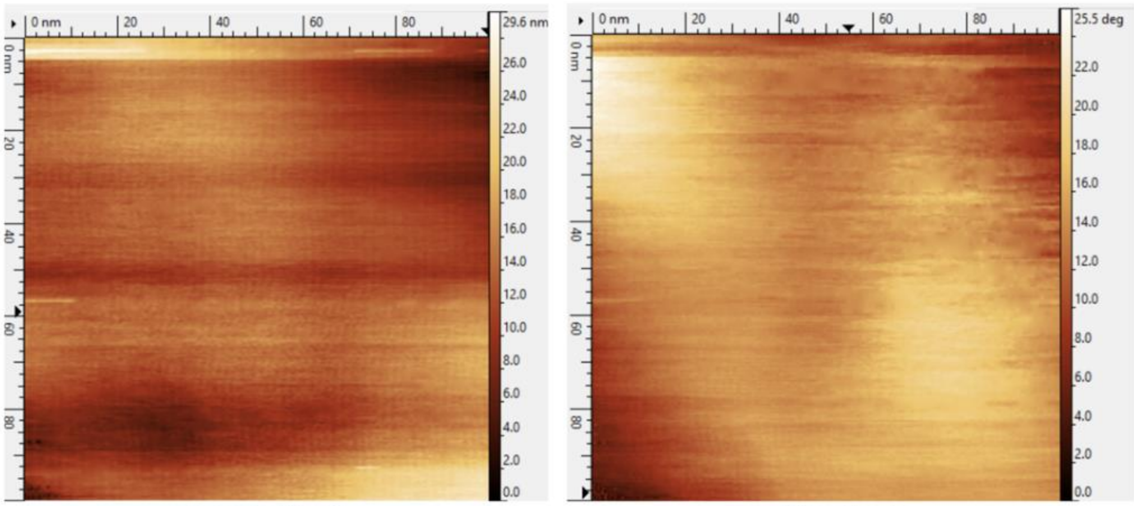

Topological Image

Phase Image

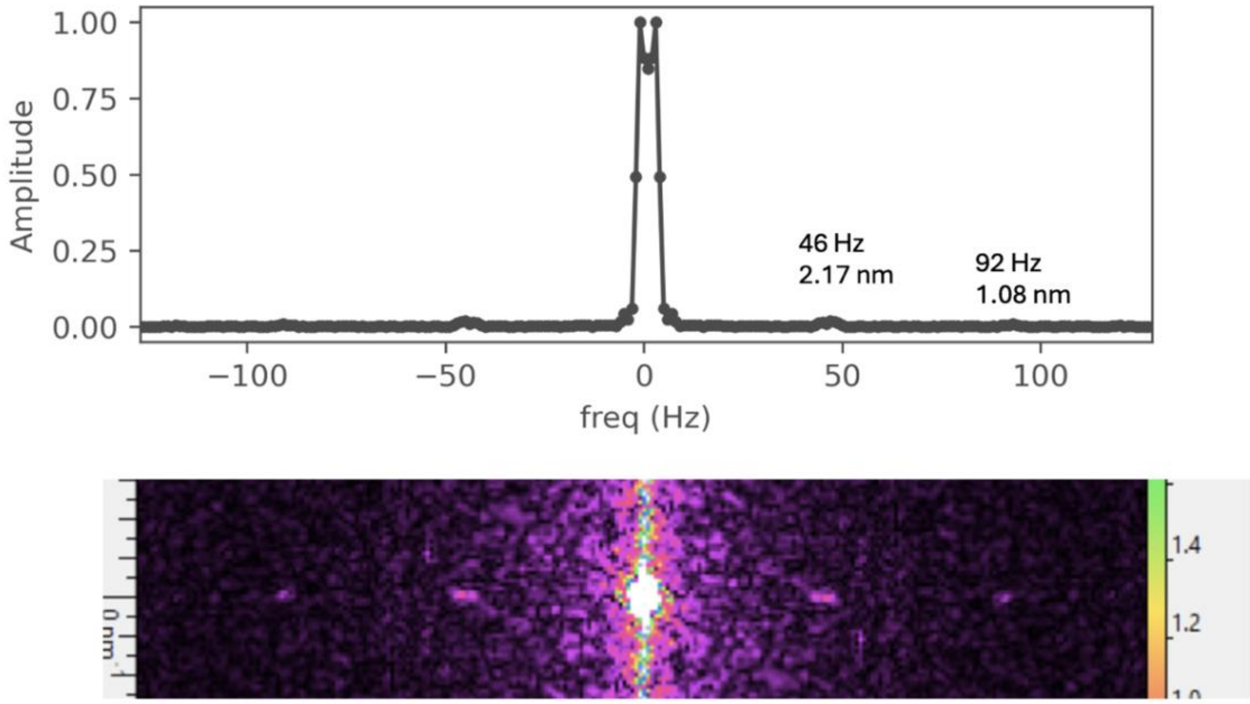

Fig 2e2 AFM spectral analysis (Spot 2)

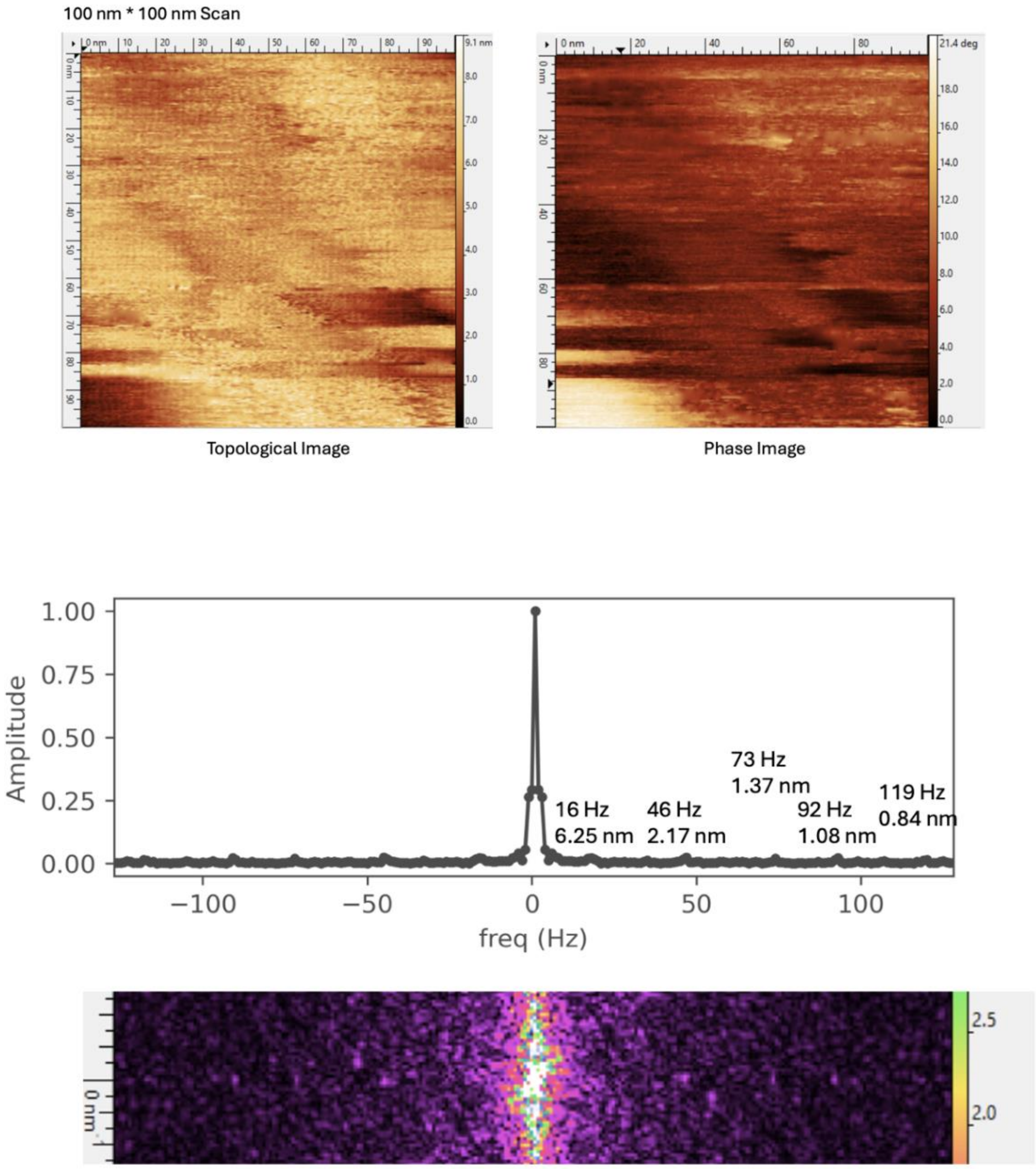

Fig 2e3 AFM spectral analysis (Spot 3)

Scan Size: 100 nm * 100 nm (0.4 nm/pixel)
Scan Rate: 0.12 Hz
Resolution: 256 * 256

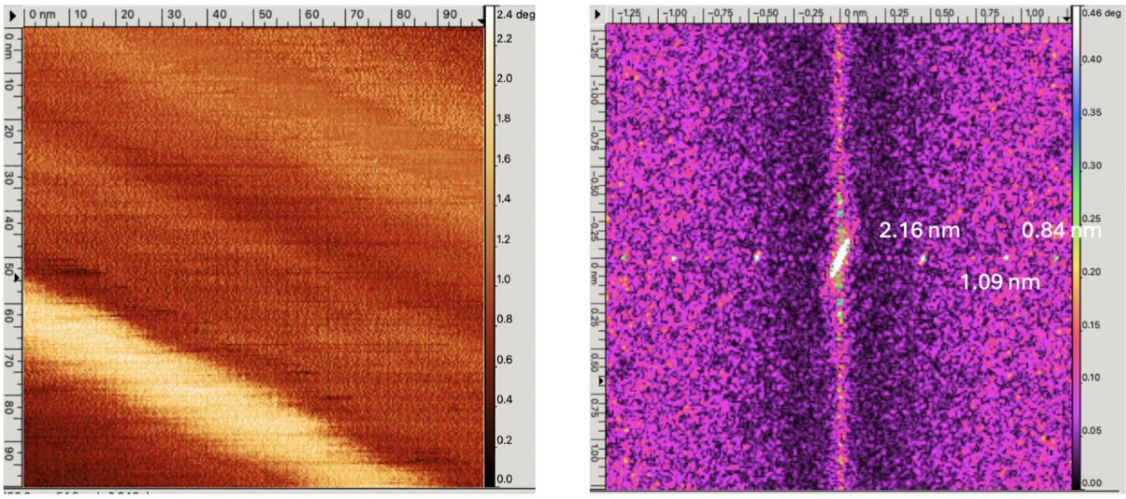

Scan Size: 400 nm * 400 nm (0.4 nm/pixel)
Scan Rate: 0.5 Hz
Resolution: 1024*1024

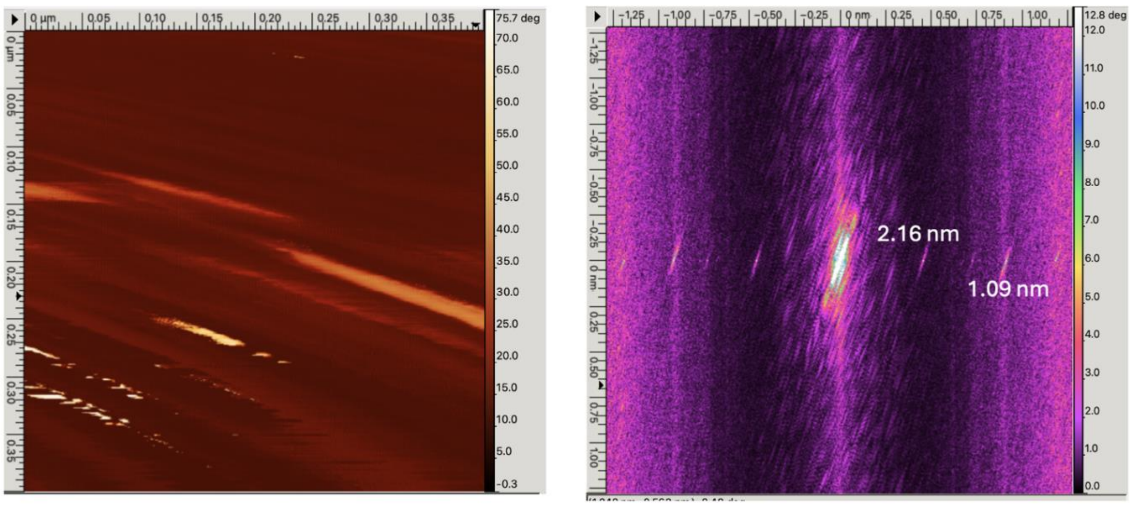

Fig 2f High-resolution AFM spectral analysis (Spot 4 & 5)

Scan Size: 400 nm * 400 nm (0.4 nm/pixel)
Scan Rate: 0.25 Hz
Image Size: 1024 * 1024

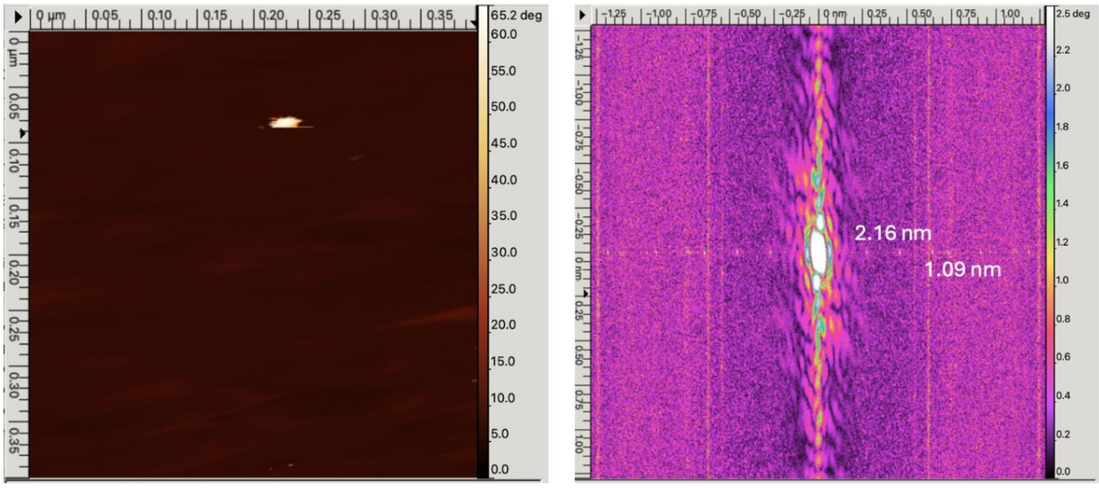

Scan Size: 70 nm * 70 nm
Scan Rate: 1 Hz
Image Size: 128* 128

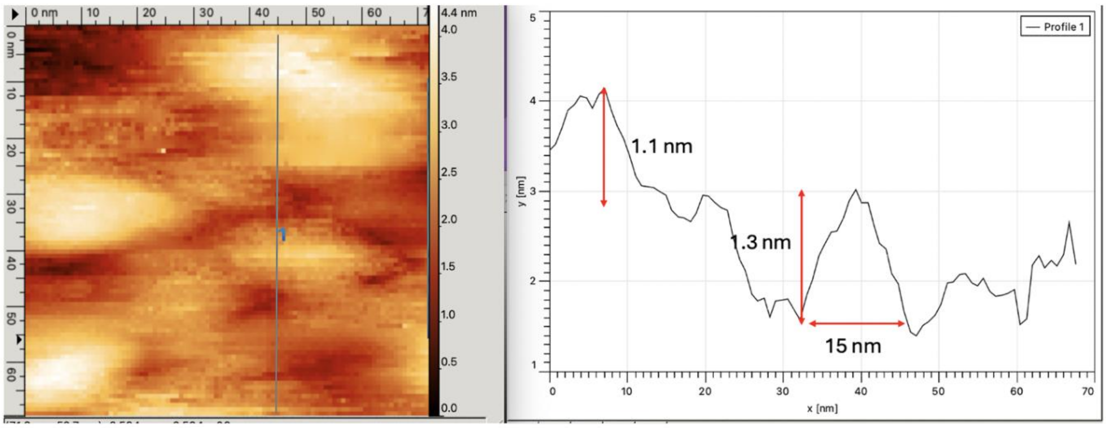

Fig 2g High-resolution AFM spectral analysis (Spot 6 & 7)

X-ray diffraction measurements on the {311} ferrite reflection yield a linear $\sin^2\psi$ dependence with slope 0.00105 (XRD Figure 2). Substitution of this value into the plane-stress relation with the elastic constants E = 180 GPa and ν = 0.30 given in the report converts to an in-plane tensile residual stress of 115 MPa . The appendix notes that delamination cracks in the same steel grade become energetically favourable only when the surface tension approaches several hundred megapascals, so the measured 115 MPa level is mechanically benign within the report's own framework.

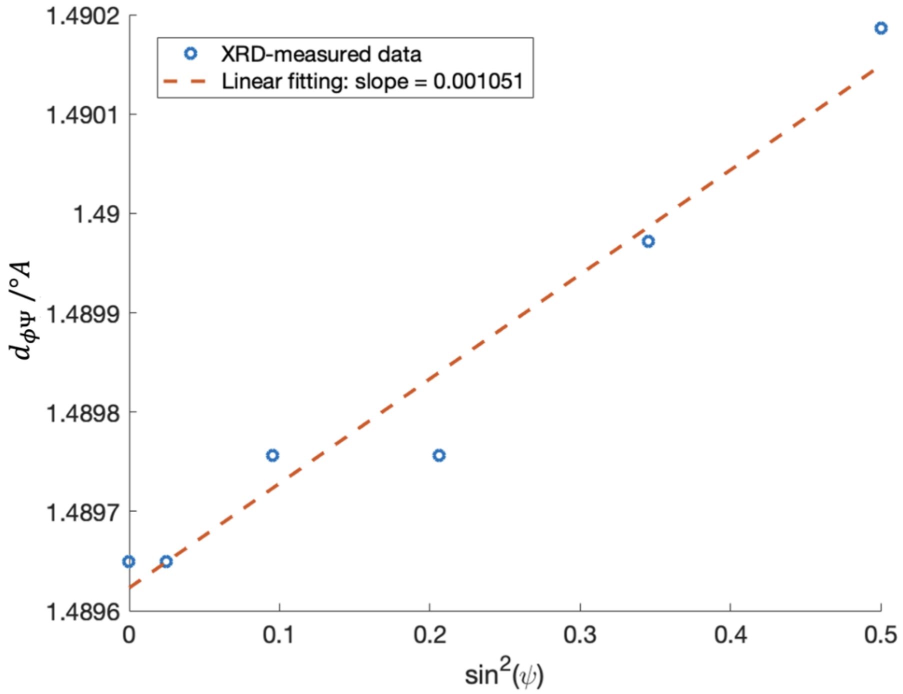

Figure 2. $\sin^2$ Ψ analysis of steel sample provided by Renox

$$\sigma_\phi = \left(\frac{E}{1+\nu}\right)\frac{1}{d_0}\left(\frac{\partial d_{\phi\Psi}}{\partial \sin^2\Psi}\right) \approx \left(\frac{200GPa}{1+0.3}\right)\frac{1}{1.4}0.0$$

Taken together, the SEM, AFM and XRD observations demonstrate that service exposure in the fullerene-bearing lubricant produces a spatially selective, 1 – 3 nm tribofilm built from ≈1 nm nanoparticles. This film blankets the highest asperity crests, converts them into load-bearing plateaux and simultaneously relaxes the residual tensile stress to a level incompatible with crack nucleation.

DISCUSSION

The multiscale dataset assembled in the Renox project demonstrates a coherent, self-consistent tribological transformation that proceeds from the nanometre to the micrometre scale. SEM evidence (*Figure 1a–1f*) proves that classical pit-initiated delamination cracks—readily visible on the deliberately unprotected track—do not arise on the surface lubricated with the modified Buckminster-fullerene additive. AFM mapping (*Figure 2a–2d*) links this macroscopic suppression of cracking to the presence of a spatially continuous 1 – 3 nm film that blankets the very asperity crests where dislocation escape and tensile-layer build-up would normally begin. Spectral analysis of seven high-resolution spots (*Figures 2e1–2g*) shows that the film is constructed from ≈1.1 nm particles, unambiguously identifying the additive itself as the building block.

The functional consequence of this self-assembly is captured by the residual-stress result: the 115 MPa tensile value obtained from the $\sin^2\psi$ plot (*XRD Figure 2*) is far below the several-hundred-megapascal threshold cited in the report's appendix as necessary for delamination crack nucleation. Because crack formation is a stress-controlled process, the measured relaxation provides a mechanistic bridge between the nanometre-scale film and the absence of cracks in the micrometre-scale SEM fields.

The report further proposes that the film forms through frictional welding of carbon cages to freshly exposed metal atoms during local flash-temperature events, while the outermost layer retains rotational mobility and therefore acts as a nano-bearing. This model rationalises the "autonomous micro-asperity flattening" seen in *Figure 1e–1f*: as each sliding pass melts or softens only the extreme asperity tips, the nanoparticles fuse into those tips, broaden them, and renew the rolling interface for the next pass, thereby producing simultaneous smoothing and protection.

All observations were made on the same wear scar, ensuring that the causal chain—nanoparticle deposition → film growth → stress relaxation → crack suppression—is internally closed and experimentally self-contained. While the investigation is necessarily post-mortem, the project notes that in-situ diffraction and spectroscopy are planned for future phases to trace film kinetics in real time; nevertheless, the present data suffice to substantiate the core mechanism identified in Section 6 of the report: *a friction-driven, self-regenerating carbon–metal nanofilm delivers both anti-wear and restorative functionality to steel surfaces.*

CONCLUSION

Comprehensive multiscale characterisation of Renox's modified C_{60}-NP lubricant system confirms the formation of a one-to-two-layer nanofilm that conforms to steel asperities and transforms their mechanical response. SEM demonstrates the elimination of pit-to-crack evolution; AFM resolves a contiguous 1–3 nm coating rooted in 1.08–1.10 nm particles; XRD quantifies a residual-stress state (115 MPa) incompatible with delamination crack nucleation. Together these results validate the dual action of the additive: (i) protective—by lowering friction and residual tension; and (ii) restorative—by continuously welding nanoparticle material into emerging defects. The study provides a rigorous experimental foundation for commercial adoption of this friction-driven self-assembly mechanism as a viable alternative to conventional ZDDP-based chemistries for high-load, cyclic or intermittently lubricated machinery.

REFERENCES

Jiang, Z., Sun, Y., Liu, B., Yu, L., Tong, Y., Yan, M., ... & Li, W. (2024). Research progresses of nanomaterials as lubricant additives. *Friction*, *12*(7), 1347-1391.

Spikes, H. (2025). Mechanisms of ZDDP—An Update. *Tribology Letters*, *73*(1), 38.

Yu, Z., Zhou, M., Liu, R., Wang, Y., & Zhang, X. (2025). Carbon nanomaterials as additives in lubricating oils for tribological applications: A review. *Diamond and Related Materials*, 112384.

Yu, H. H., Shrotriya, P., Gao, Y. F., & Kim, K. S. (2007). Micro-plasticity of surface steps under adhesive contact: Part I—Surface yielding controlled by single-dislocation nucleation. *Journal of the Mechanics and Physics of Solids*, *55*(3), 489-516.

Hurtado, J. A., & Kim, K. S. (1999). Scale effects in friction of single–asperity contacts. I. From concurrent slip to single–dislocation–assisted slip. *Proceedings of the Royal Society of London. Series A: Mathematical, Physical and Engineering Sciences*, *455*(1989), 3363-3384.

Gao, Y. F., Bower, A. F., Kim, K. S., Lev, L., & Cheng, Y. T. (2006). The behavior of an elastic–perfectly plastic sinusoidal surface under contact loading. *Wear*, *261*(2), 145-154.

Li, Q., & Kim, K. S. (2008). Micromechanics of friction: effects of nanometre-scale roughness. *Proceedings of the Royal Society A: Mathematical, Physical and Engineering Sciences*, *464*(2093), 1319-1343.

Hurtado, J. A., & Kim, K. S. (1999). Scale effects in friction of single–asperity contacts. I. From concurrent slip to single–dislocation–assisted slip. *Proceedings of the Royal Society of London. Series A: Mathematical, Physical and Engineering Sciences*, *455*(1989), 3363-3384.

Hurtado, J. A., & Kim, K. S. (1999). Scale effects in friction of single–asperity contacts. II. From concurrent slip to single–dislocation–assisted slip. *Proceedings of the Royal Society of London. Series A: Mathematical, Physical and Engineering Sciences*, *455*(1989), 3385-3400.